International Journal of Modern Manufacturing Technologies
ISSN 2067–3604, Vol. XVII, No. 2 / 2025
https://doi.org/ 10.54684/ijmmt.2025.17.2.51

EFFECT OF CONSTRAINED GROOVE PRESSING ON GRAIN REFINEMENT, MECHANICAL PROPERTIES, AND CORROSION RESISTANCE OF AA5083 ALUMINUM ALLOY

Manh Hung Le[1], Manh Tien Nguyen[2], Truong An Nguyen[2], Tam Ho[3], Xuan Diep Nguyen[2], Van Vu Phan[1]

[1]Vietnam Defence Industry, Ha Noi, Viet Nam
[2]Faculty of Mechanical Engineering, Le Quy Don Technical University, Ha Noi, Viet Nam
[3]Factory A34, Air Defence - Air Force, Ha Noi, Viet Nam

Corresponding author: Manh Tien Nguyen, manhtiennguyen84@lqdtu.edu.vn

Abstract: The Al-Mg system is extensively utilized in engineering applications due to its inherent corrosion resistance and moderate strength levels. However, further enhancement of these properties is essential for their effective deployment in demanding industrial environments. In this context, severe plastic deformation (SPD) methods have emerged as a promising approach for microstructural refinement and property improvement. The present study focuses on evaluating the effect of the constrained groove pressing (CGP) technique on the structural characteristics, mechanical performance, and corrosion behavior of AA5083 alloy. Experimental results demonstrate a progressive refinement in grain size, with a reduction from an original average of 50 μm to approximately 3 μm following four CGP cycles. This microstructural modification is accompanied by notable increases in microhardness and tensile strength, approximately 49% and 32%, respectively, relative to the undeformed material. Corrosion resistance, quantified via electrochemical analysis, also exhibited a substantial improvement, with a corrosion rate reduction indicating an enhancement of around 26%. These results underscore the effectiveness of CGP as a viable processing route for significantly upgrading the functional properties of AA5083, thereby supporting its application in high-performance and corrosion-sensitive industrial sectors.

Keywords: severe plastic deformation (SPD), constrained groove pressing (CGP), grain refinement, mechanical properties, corrosion resistance, AA5083 alloy.

1. INTRODUCTION

Aluminum–magnesium (Al–Mg) alloys are classified as non-heat-treatable wrought materials and are extensively used in engineering applications because of their superior corrosion resistance, excellent weldability, and balanced mechanical properties. The presence of magnesium, typically between 3 and 5 wt.%, enhances the alloy's strength primarily through solid-solution strengthening. These alloys also demonstrate favorable formability, enabling their use in various plastic deformation processes such as rolling, extrusion, and deep drawing. The combination of mechanical performance and corrosion resistance makes Al-Mg alloys suitable for marine structures, transportation components, and chemical processing equipment [1-3].

Although aluminum alloys offer advantages such as excellent corrosion resistance and low density, they present several limitations when applied in seawater environments. A major concern is their relatively limited resistance to stress corrosion cracking and crevice corrosion, particularly in regions subjected to high mechanical loads or confined spaces. Aluminum alloys are also susceptible to galvanic corrosion when in contact with dissimilar metals in marine conditions, which can significantly reduce service life. Moreover, the mechanical strength of aluminum alloys is generally lower than that of certain steels, restricting their use in applications requiring high load-bearing capacity. Additionally, their thermal resistance and wear resistance are inferior compared to other metallic materials such as titanium or stainless steel, limiting their suitability for more severe service conditions. Finally, maintenance costs may increase due to the need for specialized surface treatments to enhance long-term durability and corrosion protection [4].

Severe plastic deformation (SPD) is a class of metalworking processes that introduces very large plastic strains into materials, while the overall shape and dimensions change only negligibly [5,6]. The primary objective of SPD is to produce ultrafine-grained or even nanocrystalline structures, which are known to enhance mechanical strength, ductility, and thermal stability. Unlike conventional deformation methods, SPD techniques achieve grain

refinement predominantly through the activation of dislocation mechanisms and dynamic recrystallization. Several SPD routes, including Equal Channel Angular Pressing (ECAP), Multidirectional Forging (MDF), High Pressure Torsion (HPT), and Constrained Groove Pressing (CGP), have attracted significant research interest because of their efficiency in grain refinement and their suitability for bulk material processing [7–10]. These processes enable significant modifications in the internal structure of metallic materials while preserving their macroscopic shape, making them suitable for industrial applications. SPD-treated materials often exhibit a remarkable combination of strength and toughness, surpassing the typical trade-off observed in coarse-grained counterparts. Furthermore, the refinement of microstructure can contribute to improved surface properties, including corrosion resistance and wear behavior. Recent developments in SPD research have focused on hybrid techniques and process optimization to address limitations such as strain inhomogeneity and processing time. As a result, SPD continues to evolve as a versatile platform for tailoring material performance to meet the demands of advanced engineering systems.

Numerous studies have highlighted the role of the CGP technique in refining the microstructure of aluminum alloys, thereby significantly enhancing their mechanical properties and corrosion resistance. The CGP process promotes intensive grain fragmentation, producing finer grains that contribute to improved strength and hardness of the material [11-13]. Repeated CGP cycles have been shown to progressively enhance tensile properties by increasing dislocation density and activating grain boundary strengthening mechanisms. Furthermore, CGP improves the surface oxide layer, enhancing corrosion resistance by forming a more uniform and stable protective film. The degree of improvement depends on specific processing conditions and alloy composition. Ren-jie FAN et al [14] demonstrated that the CGP technique significantly refines the microstructure of AA6063 aluminum alloy, reducing the grain size from approximately 100 μm to the submicron scale. This refinement leads to a marked increase in hardness and improved hardness uniformity with successive passes. Moreover, CGP processing enhances corrosion resistance by promoting the formation of a more stable passive film and altering the morphology of intermetallic precipitates that typically act as localized corrosion initiation sites. A. Sajadi et al [15] conducted both experimental and numerical investigations of the CGP process applied to 2-mm-thick commercial pure aluminum over four pressing passes. The results showed that hardness and tensile strength increased rapidly during the first three passes due to strain hardening and grain refinement, followed by a slight decrease in the fourth pass as a result of strain softening and the formation of microcracks. Finite element simulations indicated that the equivalent plastic strain was not uniformly distributed, with lower values observed at the surface and near the die tooth regions. In addition, the changes in the mechanical properties of AA7075 aluminum alloy during the CGP process were investigated by Shahin Heidari et al [16]. The study shows that the constrained groove pressing (CGP) process significantly refines the microstructure of 7075-T6 aluminum alloy, reducing the initial grain size from approximately 60 μm to about 270 nm after four pressing passes. This substantial grain refinement results in an increase in hardness from 157 HV to 254 HV, while the yield strength and tensile strength rise by 38% and 34%, respectively, compared to the annealed sample. However, the elongation decreases markedly to around 40%, indicating a reduction in ductility with increasing pressing passes. These findings indicate that CGP is an effective technique for tailoring the microstructure and functional properties of industrial aluminum alloys.

This study aims to systematically investigate the effects of the CGP process on the microstructure, mechanical properties, and corrosion behavior of the AA5083 aluminum alloy. The research will involve performing multiple CGP passes to achieve grain refinement and evaluate corresponding changes in microhardness and tensile strength. Corrosion resistance will be assessed through electrochemical methods to quantify improvements in corrosion rate and passive film stability. The findings are expected to contribute to the development of aluminum alloys with enhanced durability and mechanical efficiency for use in harsh environments.

2. MATERIALS AND METHODS

The experimental material consisted of cold-rolled AA5083 aluminum alloy sheets, which were machined into rectangular specimens with dimensions of 50 mm × 40 mm × 2 mm. The nominal chemical composition of the alloy is listed in Table 1. To prepare the material for SPD, a heat treatment was applied to reduce internal stress and promote microstructural uniformity. The annealing procedure consisted of heating the specimens at 450 °C for one hour to allow sufficient recovery and partial recrystallization. Upon completion of the annealing treatment, the specimens were gradually furnace-cooled to 260 °C to mitigate steep thermal gradients, followed by natural cooling to ambient temperature. This thermal regimen facilitated the stabilization of the microstructure and minimized the potential for distortion during subsequent mechanical processing [17].

Table 1. Chemical composition of AA5083 aluminum alloy (wt.%)

Si	Fe	Cu	Mn	Mg	Cr	Zn	Ti	Al
0.4-0.7	≤0.4	≤0.1	0.4-1.0	4.0-4.9	0.05-0.25	≤0.25	≤0,15	Balance

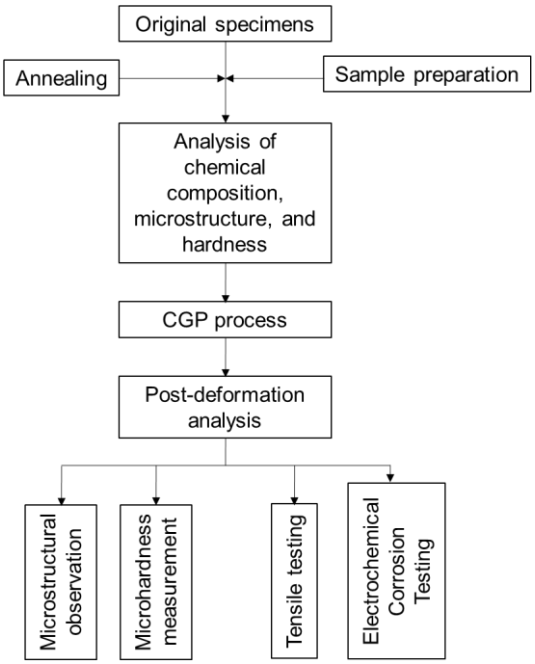

Fig. 1. Schematic of the experimental procedure

Figure 1 presents a schematic overview of the experimental procedure conducted in this study. The initial annealing of the specimens was conducted using a Nabertherm LH 120/13 resistance furnace to ensure uniform thermal treatment. The chemical composition of the alloy was determined using a LAB LAVM11 optical emission spectrometer to verify the consistency of alloying elements. Microstructural observations before and after CGP processing were conducted with AXIO A2M and AXIOVERT-25C optical microscopes. Before examination, specimens underwent surface preparation involving sequential grinding with P2000-grade abrasive paper and mechanical polishing. Keller's reagent (95 ml H_2O, 1 ml HF, 2.5 ml HNO_3, 1.5 ml HCl) was employed for etching to reveal the grain structure. Post-deformation analysis included microstructural evaluation, microhardness testing, tensile property measurement, and corrosion resistance assessment. Microhardness was measured along both transverse and longitudinal directions using a DURAJET hardness tester. Tensile specimens were prepared in accordance with ISO 6892-1:2016, and tensile tests were conducted at ambient temperature using a Devotrans DVT FU/RDNN 50kN-CKS testing system. Electrochemical corrosion behavior was evaluated by performing potentiodynamic polarization tests in a sodium chloride (NaCl) solution. A three-electrode cell configuration was used, with the specimen serving as the working electrode. Electrochemical corrosion measurements were performed using a PGSTAT302N system. The polarization curves were analyzed to quantitatively extract the corrosion potential (Ecorr), corrosion current density (Icorr), and the associated corrosion rate. All tests were carried out at room temperature under stabilized open-circuit potential conditions.

The grain refinement process was carried out using a CGP technique, which introduces SPD into sheet materials through repetitive in-plane shear, while preserving their overall shape. This method relies on a repeated sequence of pressing operations involving alternating grooved and flat dies to impose controlled shear strains across the sheet. Each full CGP cycle comprises four operations. Initially, the flat sheet is compressed between two grooved dies that induce shear deformation via inclined surfaces. Next, a flattening step is performed using flat dies to remove the resulting surface undulations. Before the third stage, the specimen is translated laterally by a distance equal to the groove pitch, which ensures that regions not previously deformed are exposed to shear in the subsequent grooved pressing. This is followed by a second flattening operation, concluding one CGP cycle and restoring the specimen to its original geometry.

The sequential steps of the CGP cycle are schematically illustrated in Figure 2. In the initial configuration (Figure 2a), the undeformed sheet is positioned between the upper and lower dies. The first step (Figure 2b) involves pressing the sheet between grooved dies to initiate localized shear deformation. Subsequently, the second step (Figure 2c) employs flat dies to eliminate surface undulations and restore geometric flatness. Before the third step,

the specimen is laterally displaced by a distance corresponding to the groove pitch, enabling previously unstrained regions to align with the die grooves (Figure 2d). A second grooved pressing is then applied in the third step (Figure 2e) to introduce additional shear strain. Finally, the fourth step (Figure 2f) involves a second flattening operation to complete the cycle. This systematic approach facilitates homogeneous strain distribution and promotes the accumulation of SPD across the material. The CGP process was applied in 1 to 4 cycles using a YH32 hydraulic press rated at 100 tons. Two dedicated die sets were designed and fabricated to perform groove indentation and subsequent flattening within each cycle (as illustrated in Figure 3).

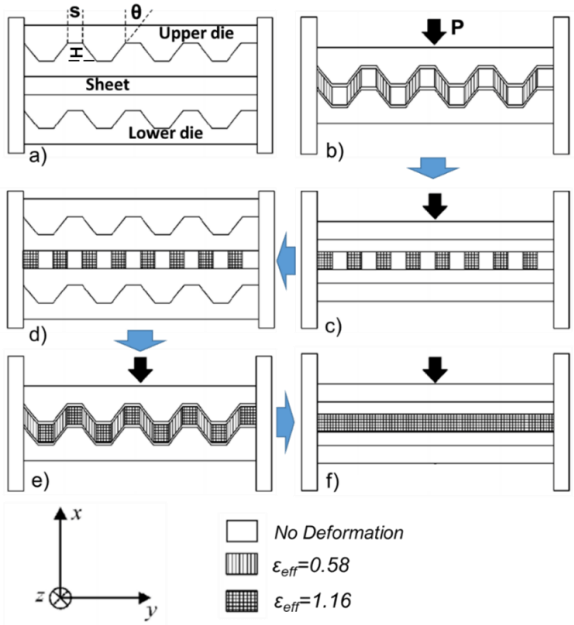

Fig.2. Schematic illustration of the CGP cycle: (a) initial step (pre step); (b) first step (grooving a flat blank); (c) second step (flattening the grooved blank); (d) rotating the blank; (e) third step (second grooving of the flat blank); (f) fourth step (final flattening of the grooved blank).

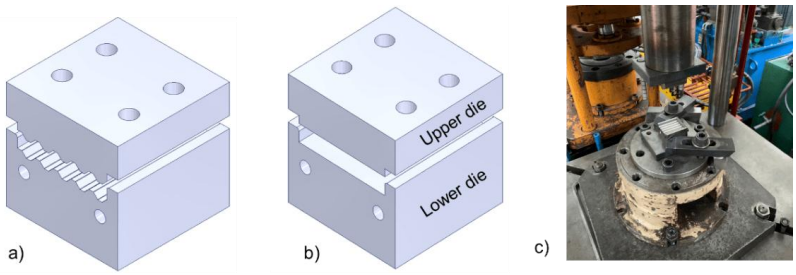

Fig. 3. Design of the grooving (a) and flattening (b) dies for the CGP process and experimental process (c)

3. RESULTS AND DISCUSSION

The initial geometry and the post-deformation shape of the billet after the first CGP cycle are illustrated in Figure 4. The dimensions of the specimens after each CGP cycle are reported in Table 2. The width of the specimens was constrained in both directions and therefore remained unchanged. The specimen length exhibited only minor variations because the deformation predominantly occurred along the groove profiles of the dies. Thickness measurements before and after pressing showed very small dimensional deviations, indicating high geometric stability in the thickness direction. The die configuration effectively restricted outward material flow, leading to strain localization along the die's grooves and inclined interfaces. As a result, a distinct wavy morphology emerged on the surface, indicating uniform shear deformation during processing.

Throughout the initial pressing step, the material responded with substantial plastic flow, closely conforming to the die geometry. At this stage, the form-filling capability was generally acceptable; however, slight void formation was noted at the base of the grooves due to incomplete filling. As deformation cycles were repeated, accumulated strain facilitated better cavity conformance and reduced the extent of unfilled regions. By the fourth pass, however, surface cracking was detected at the crest regions of the grooves. These defects were likely caused by stress accumulation in restricted flow zones, combined with increased work hardening, suggesting a need for further optimization of the forming parameters to enhance material durability under large strain.

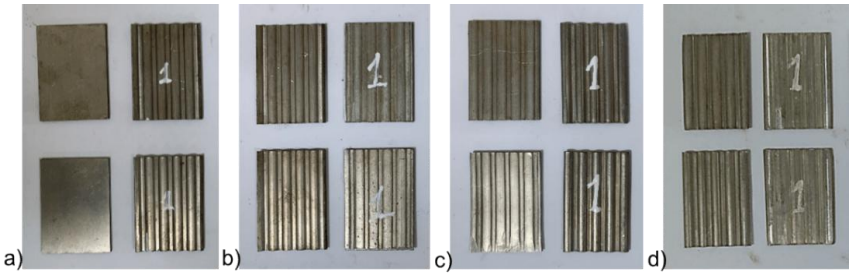

Fig. 4. Original specimens and deformed specimens after one cycle of the CGP process
a) first step; b) second step; c) third step; d) fourth step

Table 2. Specimen dimensions after each CGP cycle

Specimen	Length, [mm]	Width, [mm]	Thickness, [mm]	Flatness, [mm]
Original	50±0.02	40±0.02	2±0.02	≤0.1
After CGP cycle 1	50.08±0.02	40±0.02	1.9±0.02	≤0.1
After CGP cycle 2	50.1±0.02	40±0.02	1.9±0.02	≤0.1
After CGP cycle 3	50.12±0.02	40±0.02	1.9±0.02	≤0.1
After CGP cycle 4	50.16±0.02	40±0.02	1.9±0.02	≤0.1

The starting material consisted of rolled aluminum alloy sheets, characterized by elongated grains due to previous deformation. To ensure a homogeneous microstructure before testing, the specimens underwent a recrystallization annealing treatment. This thermal step allowed for the development of equiaxed grains with distinct boundaries and eliminated residual internal stresses. The resulting starting structure, as depicted in Figure 5a, was characterized by relatively coarse, homogeneously distributed grains, which provided a suitable baseline for observing the effects of CGP-induced strain.

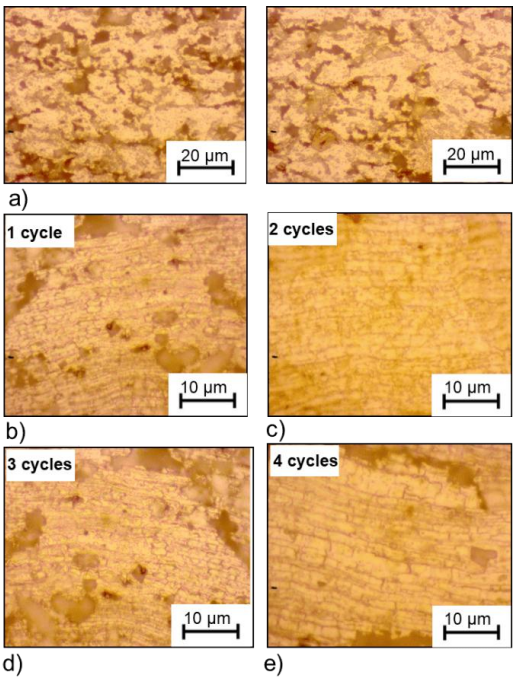

Fig. 5. Optical microstructures of AA5083 specimens after successive CGP cycles
(a) original specimen, (b) after 1 cycle, (c) after 2 cycles, (d) after 3 cycles,
and (e) after 4 cycles

Detailed analysis of the microstructure following each CGP cycle demonstrated a clear trend of grain size reduction and increased uniformity. The cumulative shear strain introduced by successive passes facilitated progressive fragmentation and rearrangement of the grains. To accurately assess this evolution, grain size measurements were conducted using image processing techniques. Due to the irregularity of the deformed grains, the conventional linear intercept method was unsuitable. Therefore, grain dimensions were instead quantified using calibrated image analysis software (ImageJ), by outlining grain boundaries and calculating equivalent grain diameters across multiple fields of view for statistical reliability. The measurement process was conducted at multiple locations on the microstructural images. The specimens were examined for microstructure in the direction

perpendicular to the grooves. This is the direction in which the deformed grains are continuously sheared through the CGP cycles, revealing the grain refinement process more clearly.
The measured values showed a significant decrease in grain size as the number of deformation cycles increased. The annealed specimen had an average grain size of approximately 49.08 µm, with individual measurements ranging from 31.04 µm to 65.93 µm. After one cycle, the average dropped markedly to 12.98 µm, indicating a notable degree of structural refinement (Figure 5b). Continued processing further reduced the grain size to 8.96 µm, 5.68 µm, and ultimately 3.27 µm after the second, third, and fourth cycles, respectively (Figure 5c-e). While each step contributed to further refinement, the most pronounced change occurred during the first deformation cycle, after which the rate of grain size reduction gradually diminished. This phenomenon implies the onset of a saturation regime, where dynamic recovery and grain boundary stabilization limit further refinement.
The CGP technique proves highly effective in promoting grain refinement and enhancing microstructural homogeneity in aluminum alloys. The extent of refinement was directly linked to the level of plastic strain introduced by the number of processing cycles. These results confirm the potential of CGP as a viable SPD method for modifying microstructure and improving the mechanical performance of metallic materials.

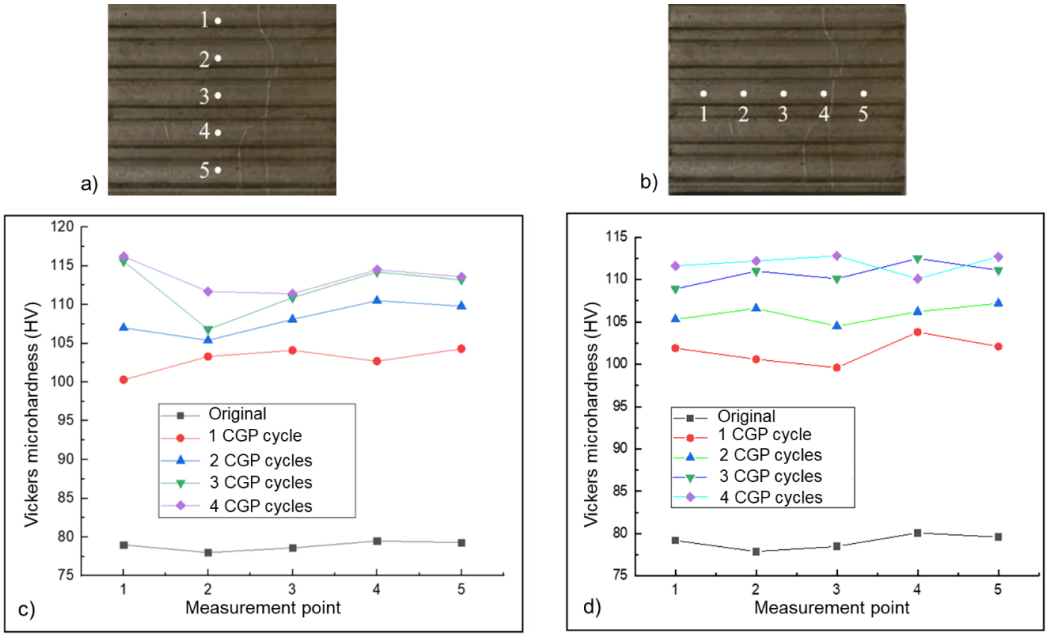

Fig. 6. Measurement positions in the transverse direction (a) and longitudinal direction (b), and the corresponding microhardness results in the transverse (c) and longitudinal (d) directions after successive CGP cycles.

Microhardness testing was performed on the original specimen to establish a baseline for comparison. After each cycle of the CGP process, the microhardness of the deformed specimens was measured along both the transverse and longitudinal directions relative to the specimen axis. The locations of the measurement points are illustrated in Figures 6a and 6b, whereas the associated microhardness values are displayed in Figures 6c and 6d. The original specimens exhibited relatively uniform microhardness values, ranging from 78 to 80 HV. The microhardness values at different positions along both the longitudinal and transverse directions showed negligible variation. The variation between the maximum and minimum microhardness values was below 15%. Microhardness measured along the longitudinal direction displayed higher uniformity compared to that along the transverse direction at corresponding specimen locations following the CGP cycles. Accordingly, this section focuses on analyzing the influence of CGP cycles on the microhardness distribution along the transverse direction of the deformed specimens.
In the first CGP cycle, the maximum measured microhardness reached 104.3 HV, representing an increase of approximately 33.72% compared to the original specimens. During the second CGP cycle, the highest microhardness value recorded at the measured positions was 110.2 HV, indicating an increase of 41.28% compared to the undeformed specimen. This continued improvement in hardness is attributed to the progressive plastic deformation introduced by the CGP process. In the third cycle, the maximum microhardness further rose to 115.6 HV, corresponding to a 48.2% increase. By the fourth cycle, the peak microhardness reached 116.2 HV, marking a total increase of 48.97% relative to the original specimen.
The results indicate that the most pronounced enhancement in microhardness occurred during the original CGP cycle, likely due to the substantial introduction of strain and microstructural refinement in the early stage of

deformation. Although subsequent cycles contributed to further increases, the rate of hardening gradually declined, suggesting a saturation trend in the material's response. Notably, the gain in microhardness from the third to the fourth cycle was marginal, approximately 1% implying that the material was approaching a stable microstructural condition where additional deformation had limited influence on microhardness.
Such a tendency, where the most significant property changes are observed in the early deformation cycles, is consistent with behaviors reported for other SPD methods. Continued processing beyond the original stages often leads to microstructural homogenization rather than further hardening [18].
The results of ultimate tensile strength and relative elongation measurements for the original specimen and the specimens after successive CGP cycles are presented in Table 3.

Table 3. Tensile strength and elongation of specimens after CGP cycles

No.	Specimen	Ultimate Tensile Strength, σ_b (MPa)	Elongation, δ (%)
1	Original	285.5	12.72
2	After CGP cycle 1	356.4	11.43
3	After CGP cycle 2	365.2	10.2
4	After CGP cycle 3	376.8	8.77
5	After CGP cycle 4	378.2	7.63

In its as-received condition, the material exhibited a tensile strength of 285.5 MPa and a relatively high elongation of 12.72%, indicating good ductility. After undergoing the first CGP cycle, the tensile strength increased noticeably to 356.4 MPa, which corresponds to a gain of approximately 24.8%. Meanwhile, elongation decreased to 11.43%, reflecting the initiation of strain hardening mechanisms.
Further CGP processing led to a continued enhancement in strength. Specifically, after the second, third, and fourth cycles, the tensile strength values rose to 365.2 MPa, 376.8 MPa, and 378.2 MPa, respectively. These improvements are likely due to the cumulative effects of plastic deformation, dislocation multiplication, and microstructural refinement. After four CGP cycles, the tensile strength exhibited an overall increase of approximately 32.4% relative to the initial state. In contrast, ductility progressively decreased with the increasing number of CGP cycles. The elongation values dropped to 10.20%, 8.77%, and 7.63% after the second, third, and fourth cycles, respectively. This inverse relationship between strength and ductility is characteristic of SPD techniques, in which the enhancement of strength is typically accompanied by a reduction in plastic formability, resulting from grain boundary strengthening and limited dislocation mobility
The first CGP cycle had the most pronounced impact, resulting in the largest change in both tensile strength and ductility. Although additional cycles still contributed to strengthening, the rate of improvement decreased, suggesting that the material was approaching a saturation point in terms of work hardening. Simultaneously, the continued reduction in elongation underscores the inherent trade-off between strength and ductility during SPD processing. These findings highlight the effectiveness of the CGP process in strengthening aluminum alloys while also confirming the typical mechanical behavior associated with SPD methods.
The corrosion resistance of AA5083 aluminum alloy after CGP processing was assessed via potentiodynamic polarization tests. The specimens were immersed in a sodium chloride (NaCl) solution, and a potential sweep was applied to determine the corrosion potential, corrosion current density, and corrosion rate. The resulting electrochemical parameters are summarized in Table 4 and illustrated in Figure 7.
The results reveal a noticeable improvement in the corrosion resistance of the AA5083 alloy with increasing numbers of CGP cycles. The corrosion rate decreased from 0.27954 mm/year for the as-received material to 0.20498 mm/year after the fourth CGP cycle, corresponding to a 26.67% reduction. Concurrently, the corrosion potential shifted in the positive direction, from -0.86808 V initially to -0.735 V after four cycles. This trend indicates a reduced tendency for anodic dissolution and, consequently, better corrosion resistance.

Table 4. Electrochemical parameters of AA5083 aluminum alloy after CGP cycles

No.	Specimen	Corrosion rate (mm/year)	Corrosion potential (V)	Corrosion current density (A/cm^2)
1	Original	0.27954	-0.86808	8.55E-06
2	After CGP cycle 1	0.24046	-0.79079	7.36E-06
3	After CGP cycle 2	0.22878	-0.76943	7.00E-06
4	After CGP cycle 3	0.21466	-0.74973	6.57E-06
5	After CGP cycle 4	0.20498	-0.735	6.27E-06

The most significant reduction in corrosion rate was observed after the first CGP cycle (approximately 14%), with subsequent cycles contributing more moderate improvements. This suggests that the primary enhancement in

corrosion behavior occurs in the early stages of severe plastic deformation. The decreasing magnitude of improvement with additional cycles points toward a saturation of structural refinement effects on corrosion behavior.

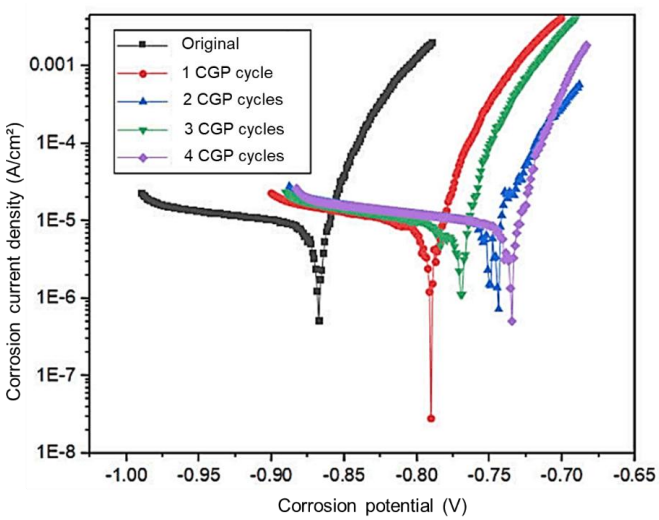

Fig. 7. Potentio dynamic polarization curves of AA5083 aluminum alloy after CGP cycles.

These improvements in corrosion performance can be closely linked to the grain refinement and homogenization occurring during CGP processing. As the material undergoes plastic deformation, the grain size becomes finer, and the grain boundary density increases. However, in aluminum alloys, particularly those with high magnesium content like AA5083, finer grains tend to support a more uniform and adherent passive oxide layer (Al_2O_3), which serves as a barrier against corrosive attack. Additionally, the CGP process helps eliminate surface defects and reduces localized micro-galvanic coupling between second-phase particles and the aluminum matrix. This decrease in microstructural heterogeneity significantly contributed to the reduction of the corrosion current density, which decreased from 8.55×10^{-6} A/cm² to 6.27×10^{-6} A/cm² following four CGP cycles.

Figure 7 illustrates the polarization curves for the AA5083 specimens. A consistent rightward shift of the anodic and cathodic branches is observed with each CGP cycle, confirming the enhancement in electrochemical stability. The decreased slope of the anodic branch after CGP processing also implies reduced susceptibility to pitting and uniform corrosion.

These findings are consistent with previous studies on SPD-processed aluminum alloys [19, 20], where grain refinement and improved passive film stability contributed significantly to enhanced corrosion resistance. It is important to note that while SPD techniques often aim to improve mechanical properties, their positive effect on corrosion behavior can be equally beneficial, especially for structural components exposed to harsh environments such as marine or aerospace applications.

4. CONCLUSIONS

This study confirmed that CGP significantly improves the microstructure and properties of AA5083 aluminum alloy. The average grain size was reduced from 50 μm to 3 μm after four CGP cycles, contributing to notable increases in microhardness and tensile strength (up to 49% and 32%, respectively). Despite a slight reduction in ductility, the alloy retained acceptable formability.

The tensile strength of the alloy increased by over 30% after four cycles, while microhardness showed nearly a 49% rise. Although ductility decreased with further deformation, the values remained within acceptable ranges for structural applications. The most significant changes were observed during the first two CGP cycles, indicating a saturation trend in both strength and microhardness with additional passes.

Electrochemical measurements indicated that CGP processing enhanced the corrosion resistance of the alloy. The corrosion rate was reduced by over 26%, accompanied by a positive shift in the corrosion potential. These enhancements are attributed to grain refinement, the formation of a more uniform passive oxide film, and the reduction in surface defects and micro-galvanic sites.

In summary, CGP offers a promising approach for simultaneously optimizing mechanical and corrosion-related properties of AA5083 without altering its geometry. These results suggest its suitability for high-performance applications in sectors such as marine, transportation, and defense, where strength, durability, and corrosion resistance are critically required.

Contributions of Authors: Manh Hung Le: Conceptualization, Methodology, Investigation, Visualization, Formal analysis, Writing - original draft, Writing - review & editing. Manh Tien Nguyen: Conceptualization, Methodology, Investigation, Visualization, Formal analysis, Writing - original draft, Writing - review & editing. Truong An Nguyen, Tam Ho, Xuan Diep Nguyen, Van Vu Phan: Conceptualization, Methodology, Investigation, Visualization, Formal analysis.
Funding source: This paper has received no external funding.
Conflicts of Interest: There is no conflict of interest.
Acknowledgment: The authors sincerely acknowledge the support of the Faculty of Mechanical Engineering at Le Quy Don Technical University for providing access to laboratory facilities and technical assistance throughout this study.

REFERENCES

[1]. X. Zhang, Y. Chen, J. Hu, (2018), *Recent Advances in the Development of Aerospace Materials*, Prog. Aerosp. Sci., 97, 22-34.
[2]. N. E. Prasad, A. A. Gokhale, and R. J. H. Wanhill, (2014), *Aluminum-Lithium Alloys: Processing, Properties, and Applications*, Elsevier, Oxford.
[3]. I.J. Polmear, (2005), *Light Alloys: From Traditional Alloys to Nanocrystals*, 4th ed., Butterworth-Heinemann, Oxford.
[4]. Ibrahim Alqahtani, Andrew Starr, Muhammad Khan, (2024), *Fracture Behaviour of Aluminium Alloys under Coastal Environmental Conditions: A Review*, Metals, 14(3), pp. 336.
[5]. J. Zrnik, S. V. Dobatkin, I. Mamuzič, (2008), *Processing of metals by severe plastic deformation (SPD)-structure and mechanical properties respond*, Metalurgija, 47(3), 211-216.
[6]. A. Azushima, (2008), *Severe plastic deformation (SPD) processes for metals*, CIRP Ann. Manuf. Technol., 57(2008), 716-735.
[7]. J.Y. Chang, A. Shan, (2003), *Microstructure and Mechanical Properties of AlMgSi alloys after Equal Channel Angular Pressing at room Temperature*, Mater. Sci. Eng., 347(1-2), 165-170.
[8]. Manh Tien Nguyen, Van Thao Le, Manh Hung Le, Truong An Nguyen, (2022), *Superplastic properties in a Ti5Al3Mo1.5 V titan alloy processed by multidirectional forging process*, Mater. Lett., 307, pp. 131004.
[9]. Alexander P. Zhilyaev, Terence G. Langdon, (2008), *Using high-pressure torsion for metal processing: Fundamentals and applications*, Prog. Mater. Sci., 53(6), 893-979.
[10]. Shantharaja M, (2013), *Mechanical Behaviour of Pure Aluminum Processed by Constrained Groove Pressing*, J. Mater. Sci. Eng., 2(5), 1-5.
[11]. A. Sajadi, M. Ebrahimi, F. Djavanroodi, (2012), *Experimental and numerical investigation of Al properties fabricated by CGP process*, Mater. Sci. Eng. A., 552, 97-103.
[12]. X. H. Wu, Y. Z. Guo, Q. C. Ruan, J. N. Lu, Y. L. Li, (2019), *Grain refinement and mechanical properties of metals processed by constrained groove pressing*, Mater. Sci. Eng., 504, pp. 012027.
[13]. H Saeidi Googarchin, B Teimouri, R Hashemi (2018), *Analysis of constrained groove pressing and constrained groove pressing-cross route process on AA5052 sheet for automotive body structure applications*, Proc IMechE Part D: J Automobile Engineering, 233(6), pp. 095440701878573.
[14]. Ren-jie Fan, Shokouh Attarilar, Mahmoud Shamsborhan, Mahmoud Ebrahimi, Ceren Göde, Hatice Varol Özkavak (2020), *Enhancing mechanical properties and corrosion performance of AA6063 aluminum alloys through constrained groove pressing technique,* Trans. Nonferrous Met. Soc. China., 30, 1790−1802.
[15]. A. Sajadi, F. Javanroodi, M. Borhani, (2012), *Experimental and Numerical Investigation of Groove Pressed UFG Pure Aluminum*, Int.J. Adv. Des. Manuf. Technol., 5(2), 1-6.
[16]. Shahin Heidari, Ahmad Afsari, (2021), *Study of Mechanical Properties of 7075 Aluminum Alloy Due to Particle Size Reduction due to Constrained Groove Pressing CGP Process*, J. Mod. Process. Manuf. Prod., 10(1), 1-14.
[17]. Mishra, R.S., and Ma, Z.Y., (2005), *Friction stir welding and processing,* Mater. Sci. Eng. R Rep., 50(1-2), 1-78.
[18]. Manh Tien Nguyen, Truong An Nguyen, (2025), *Microstructure and Microhardness of AA6061 aluminum alloy formed by cyclic expansion-extrusion process: Numerical Simulation and Experimental evaluation*, Arch. Metall. Mater., 70 (2), 625-632.
[19]. Sivaprakash Vetrivel, R. Narayanan, (2010), *Experimental investigation on corrosion behavior of rolled AA6061*, Materials Today: Proceedings, 27, 480-485.
[20]. Mariana Ilieva and Rossen H. Radev, (2016), *Effect of severe plastic deformation by ECAP on corrosion behaviour of aluminium alloy AA 7075*, Arch. Mater. Sci. Eng., 81(2), 55-61.

Received: August 15th, 2025 / Accepted: December 7th, 2025 / Paper available online: December 20th, 2025